Originally published as:

Bonn, B., von Schneidemesser, E., Butler, T. M., Churkina, G., Ehlers, C., Grote, R., Klemp, D., Nothard, R., Schäfer, K., von Stülpnagel, A., Kerschbaumer, A., Yousefpour, R., Fountoukis, C., Lawrence, M. G. (2018): Impact of vegetative emissions on urban ozone and biogenic secondary organic aerosol: Box model study for Berlin, Germany. - Journal of Cleaner Production, 176, 827-841.
DOI: https://doi.org/10.1016/j.jclepro.2017.12.164

Impact of vegetative emissions on urban ozone and biogenic secondary organic aerosol: Box model study for Berlin, Germany

Boris Bonn (a, b*), Erika von Schneidemesser (a), Tim Butler (a), Galina Churkina (c), Christian Ehlers (e, f), Rüdiger Grote (a, d), Dieter Klemp (e), Rainer Nothard (g), Klaus Schäfer (d), Albrecht von Stülpnagel (g), Andreas Kerschbaumer (g), Rasoul Yousefpour (h), Christos Fountoukis (i) and Mark G. Lawrence (a)

(a) Institute for Advanced Sustainability Studies (IASS), Berliner Straße 130, D-14467 Potsdam, Germany.
(b) now at: Chair of Tree Physiology, Albert Ludwig University, Georges-Koehler-Allee 053, D-79110 Freiburg i.Br., Germany.
(c) Geography Department, Humbold University, Unter den Linden 6, D-10099 Berlin.
(d) Karlsruhe Institute of Technologies (KIT), Institute of Meteorology and Climate Research, Department of Atmospheric Environmental Research (IMK-IFU), Division of Regional Climate Systems, Campus Alpin, Kreuzeckbahnstr. 19, D-82467 Garmisch-Partenkirchen, Germany.
(e) IEK-8, Research Centre Jülich, D-52425 Jülich, Germany.
(f) now at: Landesamt für Natur, Umwelt und Verbraucherschutz, Abtl. 4, Luftqualität, Geräusche, Erschütterungen, Strahlenschutz, Wallneyer Straße 6, D-45133 Essen, Germany.
(g) Senate Department for Urban Development and the Environment, Brückenstraße 6, D-10179 Berlin, Germany
(h) Chair of Forestry Economics and Forest Planning, Albert Ludwig University, Tennenbacher Str. 4, D-79106 Freiburg i. Br., Germany
(i) Qatar Environment and Energy Research Institute (QEERI), Hamad Bin Khalifa University, Qatar Foundation, Doha, Qatar.

* Corresponding author: Boris Bonn, Boris.Bonn@ctp.uni-freiburg.de,

Present address: Chair of Tree Physiology, Institute for Forest Sciences, Albert Ludwig University, Georges-Koehler-Allee 053, D-79110 Freiburg i.Br., Germany.

Keywords: urban vegetation, air pollution, ozone, aerosol particles, box model

Abstract

Tropospheric ozone and particulate matter affect human health and cause vegetation stress, dysfunction and damages. In this study we investigate the effect of increasing urban vegetation i.e. tree species on atmospheric chemistry, a potential urban management strategy to counteract high levels of local pollutants such as ozone, OH and PM_{10} caused by e.g. traffic. We use an extended version of an atmospheric chemistry box model including detailed gas-phase chemistry, mixing layer height variation and secondary organic aerosol calculations based on observations for Berlin, Germany. It is shown to accurately simulate the observed ozone volume mixing ratios during the intensive measurement period in July 2014 (BAERLIN2014) if basic parameters such as nitrogen oxides, meteorological conditions, PM_{10} concentrations as well as volatile organic compounds (VOCs) are considered as one hour resolved datasets. Based on this setup the effects of changing present day vegetation mixture by 24 different relevant tree species and of urban greening is tested to elucidate benefits and drawbacks in order to support future urban planning. While the present day vegetation causes boundary layer ozone to decline slightly at 35°C, individual tree types alter the ozone production rate and concentration as well as the secondary organic aerosol mass in different ways. Our results suggest that trees intensively emitting isoprene such as black locust, European oak and poplar result in higher ozone and total PM_{10} concentrations than at present, while tree species emitting primarily monoterpenes such as beech, magnolia and wayfaring trees yield less of both. This is in line with the similar behaviour of OH concentration and new particle formation rates. Thus, for future urban planning including urban greening, consideration of the beneficial and harmful aspects of tree species need to ensure that citizens benefit from and are not being negatively affected by climate adaptation strategies.

1 Introduction

Tropospheric air quality, here focussed on the lowermost kilometre of the atmosphere, is of considerable concern for life (e.g. humans) and ecosystems. Air pollution, i.e. enhanced levels of dangerous gases or particles, will cause severe health issues, reduction in working capacities, human well-being and enhancement in premature mortality (Pope III. et al., 2009, Lelieveld et al., 2015).

With respect to ecosystems and agriculture Chuwah et al. (2015) found a decline in crop yields. Fares et al. (2013) associated a reduction in carbon gain and thus carbon dioxide (CO_2) uptake because of enhanced air pollutant concentrations, while Loreto and Velikova (2001) observed evidence for an enhanced sensitivity of plants to on-going toxic pollution levels such as ozone and nitrogen oxides. With respect to humans the following health issues are currently accepted for ozone: Once inhaled the ozone will penetrate into the lung and attack the alveoli, which are responsible for the oxygen-carbon dioxide exchange between the aqueous blood system and the gaseous breath. High levels of ozone will destroy the exchange area surface structure and reduce the further exchange. If this effect lasts longer than eight hours with ozone concentrations above the threshold of 60 ppb_v or 120 $\mu g/m^3$ (WHO) health related effects are expected to be significant. Other species such as nitrogen oxides – which cause similar artefacts – and volatile organic compounds (VOCs) are supposed to be absorbed by the blood system, converted to nitric acid and different forms of oxygenated nitrates and transported to organs and brain, partially causing cancer and severe damages. Because of this, certain limits or target values have been set by national and international stakeholders to prevent substantial harm. For example eight hour averaged ozone values shall stay below 75 parts per billion volume (ppb_v, ca. 150 $\mu g/m^3$) for the United States of America (US) and below 120 ppb_v (ca. 240 $\mu g/m^3$) within the European Union (EU). If any limit or target value (e.g. for ozone, nitrogen oxides and particulate matter) is violated, local city authorities need to supply action plans so that the corresponding limit or the target value is achieved in the future. Therefore, source apportionment studies of precursors and their impact on the ozone production and lifecycle are required.

For tropospheric ozone it is established that high levels are caused by elevated levels of (a) sunlight, (b) nitrogen oxides (NO_x = NO + NO_2) and (c) volatile organic compounds (VOCs) (Seinfeld and Pandis, 2006). Ambient NO_x is primarily emitted as a product of incomplete combustion such as by transport vehicles, industrial production and heating. On the contrary VOCs consist of a multitude of known and unknown different species (>1000) of anthropogenic and biogenic sources (Goldstein and Galbally, 2007). In urban areas mankind influence ozone formation and concentration by emissions of both, i.e. NO_x and VOCs. High toxic emissions of NO result in reaction with ozone molecules temporarily converting those to NO_2, which is subsequently transported outside the city boundaries to cleaner environments and reform ozone at a much higher level than before. While the elevated NO_x emissions cause a temporary decline in ozone via e.g. formation of NO_2 and organic nitrates that photolyse or degrade partially reproducing ozone (Atkinson et al., 2006; Seinfeld and Pandis, 2006), VOC emissions force an intensified formation: Ozone production is generally called “VOC limited” i.e. the more VOCs the more ozone production in this area (Winkler et al., 2002). In this framework several mitigation strategies for current and future climate effects and challenges like water scarcity, urban heat island, air pollution and carbon emissions have been developed. This requires testing benefits and disservices of individual measures (e.g. Liu et al., 2018) before application. Such strategies include modifying cities to be carbon neutral or carbon sinks by application of biochar coatings on surfaces (Maroušek et al., 2017) or urban greening (Affolderbach and Schulz, 2017) such as “a million new urban trees” (McPherson et al., 2011). The latter has different effects: (1) Increasing shaded areas (Leal Filho et al., 2018), (2) enhancing evapotranspiration and thus evaporation cooling and (3) filtering of urban pollutants (Liu et al., 2018). The side effect is related to the emission of biogenic VOCs (BVOCs) such as isoprene, terpenes and oxygenates, subsequently participating in the urban ozone production cycle (Calfapietra et al., 2013) as well as in aerosol particle formation by mass and number (Fu et al., 2014) (Fig. 1).

The emissions of volatiles compensate heat (Guenther et al., 2006), buffer air pollution effects (Loreto et al., 2014; Jud et al., 2016a) and biotic stresses (Faiola et al., 2015). Meanwhile this part is affected by mankind in a manifold way: First by the emission of pollutants (Ghirardo et al., 2016), second by the area management resulting in plantations in a non-natural environment on a small scale causing additional stresses such as drought and competitive species; as well as third by global and regional changes such as the so-called climate change as a result of carbon dioxide emissions and enhanced temperature fluctuations (Jud et al., 2016b). All of these issues culminate in urban areas such as tested here in Berlin, Germany (Churkina et al., 2015; 2017). This study aims to support the urban planning process in order to minimize future health and vegetation effects. Therefore we consider the ozone production in detail, including the contribution of different drivers (e.g. Karlik and Pittenger, 2016) and investigate the effect of different tree mixtures and of increased vegetation areas. We postulate that stress sensitive species with high emission rates of BVOCs will cause substantial effects on air pollutants and that the effects of strong isoprene emitters will differ notably from the ones of strong monoterpene emitters. The easiest way to investigate this is using a box model that can consider complex sets of chemical reactions, phase transfers, and particulate organic mass. This was done based on a comprehensive set of measurements conducted during the Berlin Air quality and Ecosystem Research: Local and long-range Impact of anthropogenic and Natural hydrocarbons 2014 (BAERLIN2014) campaign (Bonn et al., 2016). The BAERLIN2014 campaign included a set of stationary measurements of meteorology, trace gases and aerosol particle properties in Berlin-Neukölln from June 2nd to August 28th (von Schneidemesser et al., 2017; Geiß et al., 2017) accompanied with mobile measurements in Berlin and surrounding areas (Bonn et al., 2016) with a focus on the influence of vegetation on urban air quality.

2 Materials and methods

2.1 Box model

The box model used for this study has been described elsewhere (Butler et al., 2011) in its elementary form. It is based on the Module Efficiently Calculating the Chemistry of the Atmosphere MECCA 3.0 box model set up by Sander et al. (2011) and Butler et al. (2011) and uses the Master Chemical Mechanism of Leeds University v3.2 (MCM v3.2, Jenkin et al., 1997; 2003; Saunders et al., 2003; Bloss et al., 2005). This MCM v3.2 calculates atmospheric gas-phase reactions applying a kinetic pre-processor for efficient computation. The chemical reaction code was obtained via the website: http://mcm.leeds.ac.uk/MCM. In its former version the box model included gas-phase reactions only and NO emissions were treated to find maximum ozone production rates for the present conditions. Meteorology was idealised (i.e. clear sky) and the mixing layer height (MLH) was set constant for the time of simulation. Semi-volatile organic particulate mass formation was not considered at all and thus no partitioning of organic species was possible.

For the purpose of this study the model has been modified in such a way, so that ground based meteorological and atmospheric chemical observations of two urban background reference sites have been taken into account and semi-volatile organic aerosol mass is considered. Observations include temperature, relative humidity, solar radiation and MLH (Geiß et al., 2017). Observations of nitrogen oxides (NO and NO_2), carbon monoxide (CO), a large set of VOCs including aromatics and biogenic VOCs, and particulate matter below 10 μm in particle diameter (PM_{10}) were treated

similarly. This excludes isoprene and monoterpenes, which were considered by their biogenic emission.

2.2 Biogenic emissions, Vegetation and potential tree effects

Emission rates were calculated by the so-called Guenther approach (Guenther et al., 1995; Guenther et al., 2006), i.e. dependent on leaf/needle temperature and photosynthetic active radiation. For this, the plant surface temperature has been assumed 2 K higher than air temperature to account for the established fact, that plant surfaces display reduced albedo and increased temperatures. Please note that in this context, monoterpenes are expected to be released via two pathways in the model, i.e. online because of direct production and release (temperature and photosynthetically active radiation (PAR) dependent, i.e. isoprene like) and offline from storage pools of e.g. raisin ducts related primarily to temperature only. The contribution of on- and offline pathways to monoterpene emission was based on literature data as far as available and both contributions added in the following. If no information about the individual contributions was accessible, deciduous trees were assumed as online producers and conifers as offline i.e. temperature dependent emitters only. Since data on soil moisture were not available and is expected to differ largely across the city, the reducing effect of soil water availability was ignored. The individual emission rates were derived in grams VOC per gram dry weight biomass and hour $E_{g,i}$ and were converted to molecular concentration emission rates $E_{molec,i}$ by the following equation (Eq. 1):

$$(1) \qquad E_{molec,i} = E_{g,i} * 1h/3600\ s * 1e\text{-}12 * N_A / M_{w,i}$$

N_A represents the Avogadros number and $M_{w,i}$ the species molar mass in g/mole. In order to get the emitted amount per time step this rate was applied to the corresponding chemical compound. The compound was assumed to be instantaneously well mixed, multiplied with the model time step in seconds, the dry weight (dw) biomass of about 150 g(dw)/m^2 and divided by a vertical mixing of about 20 m, which was found to yield the best match between ozone simulations with measurements.

For evaluating the impact of vegetation and the potential influence of different vegetation types, several simulations were performed: (a) bare ground with no vegetation and no biogenic emissions present ("noBVOCs"), (b) current best fitting mixture ("reference") and (c) vegetation consisting of a single selected species only. In order to achieve the best match of simulations with the observed ozone concentration values, different vegetation types with corresponding emission source strengths have been tested for the reference simulations (b). This resulted in a best match of comparable isoprene and monoterpene emission strengths such as expected for hornbeam (*Acer pseudoplatanus*) with isoprene standard emissions $E_{isop,0}$ of 0.1 μg g(dw)$^{-1}$ h^{-1} and monoterpene standard emissions $E_{mt,0}$ of 0.0093 μg g(dw)$^{-1}$ h^{-1} (Tiwary et al., 2013) evidently because the entire ozone production and sink is best described with hornbeam for the area of interest. Because of the limitation of the chemistry scheme the calculated total monoterpene emissions were split into α- and β-pinene contributions of 40% and 60%, according to the endo- and exocyclic structures of monoterpenes based on tree species of the Berlin inventory (http://www.stadtentwicklung.berlin.de/umwelt/stadtgruen/gruenanlagen/de/daten_fakten/ downloads/ ausw_5.pdf). With respect to (c) BVOC emissions were changed completely between different tree types. Please find a list of applied basal emission rates $E_{isop,0,i}$ and $E_{mt,0,I}$, temperature

dependencies of monoterpene emissions and split into on- and offline emission with references for the species considered in the appendix (Table S1).

Since single tree type emissions of trace gases add up for all the plant species, the total effect of gaseous mixtures can be derived by the sum of individual emissions and effects weighted by their relative contributions.

2.3 Organic aerosol mass description: initially available and secondary formed approaches

Additionally to the gaseous effects partitioning of semi-volatile organic compounds was newly included in the box model. Therefore organic aerosol was taken into account using two different sources and three different approaches. The accounted sources were (A) the initially available organic aerosol (IOA) representing semi-volatile organic compounds originating from either atmospheric transport of previously formed masses or from direct emission/formation within the exhaust plume of vehicles (traffic, e.g. Ehlers et al., 2013; Ehlers, 2014) ("primary" type) and (B) the secondary organic aerosol (SOA) formation on-site by semi-volatile organic aerosol precursor species, named SOA henceforth as partitioning and link to gas-phase chemistry is considered explicit. The name "primary organic aerosol" is omitted in this context because of a simple reason, i.e. to prevent misunderstanding with primary organic particles such as primary biological or rubber debris of tyres. The organic aerosol considered here refers only to low, medium and higher volatile organic compounds always establishing a rapid equilibrium between both phases, i.e. particle and gas because of the absorption process into particle mass, which depends on temperature and available organic aerosol mass present (Pankow, 1994a and 1994b).

The entire organic aerosol partitioning process newly implemented can be summarized as follows:

(A1) IOA – structural approach

(A2) IOA – associative approach

(B) SOA - explicit approach

Those will be briefly summarized in the following.

2.3.1 Approach A - Initially available organic aerosol (IOA)

The species contributing to initially available organic aerosol (IOA), i.e. secondary organic aerosol from imported and primary sources, were not derived from specific and well-known gaseous precursors within the model chemistry, as the box model has no options to retrieve detailed sources from imported or directly emitted species and their exact source speciation remains obsolete. The volatility spectrum was derived from observations as far as available. The IOA model description was based on the volatility basis set (VBS) approach of Donahue et al. (2006) with nine volatility bins scaled logarithmically (10^{-2} $\mu g/m^3 \leq c_{sat} \leq 10^6$ $\mu g/m^3$) to a decade each.

The IOAs composition is not explicitly known and was therefore treated by two different set-ups, i.e. (A1) the structural approach and (A2) the associative approach. The structural approach considers a representative artificial compound of a certain volatility bin to react always with OH forming an organic peroxy radical (RO_2), which subsequently reacts with either HO_2 producing a hydroperoxide,

with NO yielding an organic nitrate or with a different organic peroxy radical (RO_2), forming an alkoxy radical (RO) that restructures as carbonyl compound or something similar. Each oxidation initiated by OH yields a product with an approximately ten times smaller saturation concentration c_{sat}, and is thus transferred to the next volatility bin of lower volatility except the lowest one (bin 1, $c_{sat} = 10^{-2}$ $\mu g/m^3$), which stays in there (Donahue et al., 2006; Isaacman et al., 2011). A complete list of the new compounds and the corresponding idealized reactions can be found in Tables 1 and 2. Note that while an artificial compound associated to a volatility bin can partition between both phases, the compound will nevertheless remain separate from the MCM scheme, as no oxidation down to carbon dioxide and smaller species is possible. In this approach only further functional groups can be obtained resulting in a decrease in volatility.

The 'associative approach' (A2) associates each volatility bin with a representative atmospheric compound resolved within the MCM v3.2 chemistry typical for the ambient conditions of interest (Table 3). E.g. toluene was selected for the bin of highest volatility in an urban area with notable impact of traffic emissions. While for the novel representative A1 species new chemical reaction schemes were constructed, approach A2 allowed the usage of the already existing equations within the MCM. This has the benefit of the coupling between gas- and particle-phase processes und a possible feedback. Note, the lower the volatility of a bin, the more the number of functional groups of the representative compound and the higher the degree of oxidation and the less the ability to evaporate back to the gas-phase again. Therefore the most intense feedback is to be expected for the most and medium volatile species.

2.3.2 Approach B - Secondary organic aerosol formed within the area

For new secondary organic aerosol mass formation within the urban area approach (B) was used. It considered 174 selected oxidation products of substantial tropospheric organic aerosol precursor compounds treated in the MCM v3.2. These precursor compounds were representative for anthropogenic VOCs released by fossil fuel combustion (benzene, toluene, xylenes, ethyl benzene and styrene), industrial sources and biogenic VOCs (isoprene, α- and β-pinene). The partitioning compounds considered had five to ten carbon atoms and different functionalities. For oxidation products, for which no saturation vapour pressure documentation was available, a saturation vapour pressure was estimated according to the group contribution method (Stein and Brown, 1994). Any of the products was partitioned individually between the gas- and the particle phase according to the Pankow formulation (Pankow, 1994a; 1994b and references therein). Consideration of a compound was based on two criteria, i.e. the saturation vapour pressure estimated and the responsible amount formed by the partitioning process calculated for the conditions investigated in Los Angeles and Berlin. In general, compounds with at least a molar mass of 70 g, having a saturation concentration of 10^9 molecules cm^{-3} (40 $ppt_v \approx 0.1$ $\mu g/m^3$) or less at room temperature (T = 298 K) were included in the scheme. Compounds which did not obey these limits or which did not yield substantial amounts of SOA mass (≥ 0.001 $\mu g/m^3$) were excluded. An entire list of considered compounds is provided as supporting online information.

To allow organic compounds to partition (Pankow, 1994a; 1994b) the initial organic mass and its volatility spectrum was derived from observations for the CalNex campaign at Los Angeles (USA, Parrish, 2014). This was used especially for the volatility basis set approach classifying the organic

aerosol mass in ten volatility bins to test the importance. At Berlin (Germany), where no volatility observations have been conducted yet, a simple but reasonable approach was made: 50% of PM_{10} represented primary and non-volatile sources and was assumed not to interact with tropospheric chemistry and 50% of PM_{10} to consist of semi-volatile organic compounds (such as described by Jimenez et al., 2008). For any approach partitioning - i.e. distribution between both phases - was assumed to occur instantaneously and any of the compounds were redistributed after each chemical reaction time step.

These approaches were allowed to be turned on and off separately in order to check for the individual contribution. Any of the compounds were considered as two kinetic pre-processor (KPP)-species (Sandu and Sander, 2006), i.e. the compound in the gas-phase and in the particle phase. While approach (A) split gas- and the particle-phase concentrations according to the constant bin volatility, (B) yielded varying particulate masses depending on present temperature, on total organic aerosol particle mass and on the individual compounds concentrations. Other potential aerosol chemical constituents such as (non-organic) nitrates and sulphates were not explicitly treated in this study as they do not tend to evaporate into the gas-phase easily and are not expected to influence the gas-phase concentrations of ozone and other oxidants to a significant extend.

2.4 Time frame considered

The box model used in this study has be tested for three different radiation conditions during maximum summertime ozone a priori, i.e. (1) Los Angeles (USA, 34° 3'N), (2) Berlin (Germany, 52° 31'N) and (3) Helsinki (Finland, 60° 10'N) for different times, for which measurements were available (see appendix). These comparisons were found to agree well and we will concentrate on the Berlin condition because of the studies focus. In order to investigate representative conditions for Berlin, i.e. a warm summer day with highest biogenic VOC emission rates, July 20th in 2014, which was part of the BAERLIN2014 campaign (Bonn et al., 2016; von Schneidemesser et al., 2017) with additional measurement data, was selected. At this particular day air temperature exceeded 35°C and clear sky conditions were present during most of the day. This resulted in the second highest ozone mixing ratio observed in 2014 of (94.8±0.3) ppb_v.

2.5 Meteorological parameters, trace gas concentrations and particular masses

On this particular day air temperature varied between 21.8±0.1 (early morning) and (36.1±0.1)°C (earlier afternoon) and clear sky conditions were prevailing except some minor disturbance in the early afternoon. Ozone volume mixing ratios were observed between 32.3±0.5 (early morning) and (94.8±0.5) ppb_v (3 p.m.) at our reference station, an urban background residential site of the Senate of Berlin for quantifying air pollution (BLUME MC042, Berlin-Neukölln, 52° 29' 21,98" N, 13° 25' 51,08" E). The station is situated in a residential area with a small park and several smaller cafes and shops close by. Major traffic routes were about 300 m to the west with air passage blocked by at least four level buildings in between. Nitrogen oxides (NO and NO_2) were recorded at around 0.9 and 7 ppb_v during the night and at 0.3 and 4 ppb_v in the early afternoon. Furthermore a large set of additional measurements of the BAERLIN2014 campaign (Bonn et al., 2016, von Schneidemesser et al., 2017), i.e. MLH, meteorology, inorganic and organic chemistry as well as aerosol particle

detection, was available and used to make simulations most reliable. Some VOCs were quantified online by proton transfer reaction mass spectrometry (e.g. Blake et al., 2008) every ten minutes and averaged hourly afterwards. Others were samples via stainless steel canisters and analysed by gas chromatography and mass spectrometry by the Research Centre Jülich afterwards. Meteorological measurements considered and used in the box model simulations included air temperature, relative humidity, solar radiation observed in the Botanical Garden (Berlin-Steglitz), maintained by Free University of Berlin, Meteorological Institute, which is about 10 km west to the station in Neukölln. Please find a list of parameters used, scientists and institutions responsible for in Table 4. More details about the individual measurements in Berlin-Neukölln will be available in von Schneidemesser et al. (2017).

Based on all the observations a one hour time resolved dataset (minimum resolved observation frequency of all parameters) was constructed. This dataset was read in at model start and data points have been linearly interpolated in between two corresponding values. PM_{10} values have been considered as observed, since their formation is not necessarily and exclusively local and emission from the surface and it is impossible to exactly reproduce the observed pattern. Of this particular mass, 50% was considered as organic particulate mass. Only ozone and biogenic VOC measurements were excluded. Ozone was to be calculated based on the measurements and biogenic VOCs were approximated by the emission scheme for isoprene and monoterpenes. The latter behaviour was found quite similar to observations, while exact structures could not be resolved because of the large variety of plant types in the vicinity.

Any of the calculations was run for two days. But equilibration of radical and nitrogen oxide species was found within several hours.

3 Results and Discussion

3.1 Match of simulation and observation and range of effects

Figure 2 displays the comparison of ozone observations and simulation for July 20th 2014 in Berlin. Observations and simulation start at 40 ppb_v of ozone at midnight. While the simulation shows a more rapid decrease in ozone until sunrise (ca. 6 a.m., correlation coefficient = 86.4%) it catches up with the observations around 7 a.m. and nicely follows the daily pattern of observations for the rest of the day (correlation coefficient = 97.3%). This night-time effect was observed for several days in Berlin and Los Angeles (see Fig. S1) and indicates a more intense sink described by the box model than observed or a mixing of air parcels from different background conditions. Indications for the latter are deviating NO/NO_2 ratios from measurements during that time of the day. Since this was not always observed and except this night-time the daily pattern of ozone was accurately reproduced, we kept the box model set-up unchanged for the further steps.

In this context the time range of ozone destruction or production enhancing effects is of interest. In connection with the horizontal wind speed this defines the potential area of impacts. Ozone lifetime is primarily controlled by reactions of ozone with NO and NO_2 (mean: 97.0$\pm$3.3 %, min: 91.9$\pm$0.2 %). The formation rate of ozone depends predominantly on NO_2 photolysis rate $J(NO_2)$ with its highest intensity at noon (lifetime τ of NO_2 with respect to photolysis: 132$\pm$9 s) and decreases thereafter. The previous steps, yielding NO_2, i.e. (1) organic peroxy radical (RO_2) formation via VOC+OH (OH

reactivity: ca. 0.05 - 0.4 s^{-1}) and (2) the formation of NO_2 via $NO+RO_2$ (lifetime of 1.5±1.2 s) were found significantly faster. Therefore ozone formation starts about two minutes after sunrise and the local influence declines during the lifetime of ozone ($\tau(O_3)$ = 15.9±2.6 h). Assuming a vertical mixing time of close to one hour to reach roof top and a mean wind velocity of 2.7±1.3 m/s from Northeast (fluctuations between North and East-South-East) at 10 m altitude (Berlin-Tempelhof air field, German Weather Service) a maximum distance of impact of 41±7 km was estimated, i.e. the area of entire larger Berlin and surrounding.

3.2 Influence biogenic VOC emissions

VOCs can alter tropospheric ozone chemistry in two ways. First, they can join the ozone production cycle by reacting with OH radicals forming organic peroxy radicals (RO_2) which subsequently convert NO into NO_2. In doing so they produce a hydroperoxy radical (HO_2) that reacts with NO yielding NO_2 and OH (Seinfeld and Pandis, 2006). Therefore, they will enhance the ozone production as for example the small isoprene (C_5H_8). Second, VOCs can react with ambient oxidants such as ozone forming stable products and larger RO_2 radicals (> 6 C atoms), which react with NO forming organic nitrates. In this case no NO_2 is being formed but NO_x is temporarily extracted from the ozone production. If these organic nitrates or other oxidised VOC species are less volatile SOA mass will be formed and the available VOCs for ozone production will be reduced. Thus, both processes, i.e. organic nitrate and SOA mass formation, decrease the ozone production rate. The intensity of this effect depends on concentration and size of the corresponding VOCs. Smaller compounds like isoprene contribute to the formation of ozone and produce less organic nitrates and only minor amounts of SOA. Larger compounds like monoterpenes behave differently: Notable organic nitrate concentrations and SOA mass masses are formed. The effect is demonstrated in Figure 3. Both dominant BVOC classes i.e. isoprene and monoterpenes were varied in amount and the ozone simulated is plotted against daytime and isoprene and monoterpenes, respectively. The presence of isoprene (upper graph) is apparently enhancing ozone levels. Once isoprene exceeds about 100 ppt_v the effect becomes apparent. The contrary gaseous effect can be seen for monoterpenes at similar mixing ratios. The direct monoterpene effect on ozone depends on monoterpene mixture and its reactivity with respect to ozone and OH (Atkinson et al., 2006). For this plot a simple mixture of 40% α-pinene (predominantly reacting with ozone) and 60% β-pinene (pred. reacting with OH) has been assumed. The presence of more reactive monoterpenes like limonene or terpinolene would enhance this effect (Atkinson et al., 2006). BVOCs have ambient lifetimes between minutes and hours (Seinfeld and Pandis, 2006). Therefore the effect of gaseous urban BVOCs on ambient ozone is controlled by the local plant community and its emission behaviour, but smaller compared to the NO_x effect except in parks or other green spaces of notable extend.

3.3 Influence of organic particulate matter: IOA and SOA

The total effect of the organic condensed phase (OA) adds to the gaseous effects. Organic particulate matter can have a variety of different effects on ozone production. The magnitude of the total effect depends on the OA amount present and the predominant direction of the partitioning process, i.e. uptake or release of semivolatile gases. This is controlled by the ratios of local production of OA (here named as SOA) to the emitted or transported OA, addressed as initially available organic aerosol (IOA) in the following. If the predominant direction is uptake i.e. the present OA takes up condensable organic gases (SV-VOCs with saturation concentrations $c_{sat,0}$ < 100 mg/m^3, Donahue et

al., 2006) that would otherwise contribute to the tropospheric ozone production cycle, the effect is reductive. If the predominant direction is release, the ozone formation will be enhanced. This will apply if SV-VOCs are evaporating because of cleaner conditions than at formation (Ehlers et al., 2013) and/or because of elevated temperature and saturation vapour pressures around midday and afternoon. Both processes act rather independently and are linked only by the total OA mass. But they compete for dominance i.e. evaporation of pre-existing OA with the production process of SOA via gaseous reactions of precursors such as terpenes (predominantly with ozone) or aromatics (with OH). Finally the impact on the two dominating compounds OH and HO_2 in the ozone production cycle is important. As shown in Table 3 the compounds temporarily stored in the OA phase can react with radicals in the gas-phase and at the aerosol particle surface. Larger oxygenated VOCs ($>C_5$) tend to add HO_2, RO_2 and NO, forming a less volatile compound. They act as sink for HO_2, RO_2 and NO and therefore reduce the production cycle strength. All of these effects can be seen in the simulation results.

The effect was exemplarily investigated for Los Angeles because of all the necessary datasets available. The results can be applied with some changes to other locations. The contribution of initially available OA and SOA to ambient ozone is displayed in Figure 4 for an exemplary day (June 20th). A small but notable difference exists between the blue dashed line, which indicates the behaviour of ozone without any OA, and the solid black line that shows the behaviour including both types of OA. Both additional lines for simulations with either IOA or SOA indicate the individual contributions to the OA effect on ozone development, both approaching the reference simulation in different intensities. IOA contributed to 30% and SOA to 70% to ozone reduction at maximum stage. Note in this context IOA was initialized with 15 $\mu g/m^3$. The individual importance is provided in Fig. 5, considering the different volatility basis set (VBS, Donahue et al., 2006) classes i.e. volatility sections. On the left the daily variation of the total ozone mixing ratio change is displayed for turning off single VBS sections at the initial stage. The relative contribution in the afternoon (ozone maximum) is plotted on the right. As expected the most volatile sections affect the ozone most as they are able to switch the phase and alter gas-phase chemistry easiest. VBS classes 7, 8 and 9 are calculated to contribute more than 75% to the total ozone formation effect for the compound mixture observed in Los Angeles. Those are the most important ones to get the ozone mixing ratio simulated accurately. Consequently any emitted anthropogenic IOA e.g. by traffic will either evaporate step by step after its release or will alter quickly to form less volatile material that remains in the condensed phase. However, the more details are available about the volatility structure and the chemical composition of IOA the better the simulation results. Next, the amount of IOA at simulation start was varied between 0 and 150 $\mu g/m^3$ covering the range from absolutely clean to intensely polluted conditions. The changes are plotted in Figure 6 depending on daytime and IOA concentrations for OH, HO_2 (markers for ozone production cycle) and ozone. The results demonstrate that the more IOA species evaporate the larger the OH destruction. Consequently OH concentration decreases with increasing IOA mass as the ozone production cycle cannot compensate the loss (Fig. 6, top). Interestingly HO_2 shows a different pattern, displaying a minimum in the afternoon concentration at IOA levels of about 50 $\mu g/m^3$ (Fig. 6, centre). The intense concentration around 7 p.m. marked in red is due to the development of a low, nocturnal MLH and the sudden rise in impact of the available VOC species because of a drastically reduced dilution. Evidently the ozone formation process is limited by different processes. Please note in this context that only IOA was enriched but not NO_x emissions, which would also increase if the source is primarily traffic. The behaviour of HO_2 is reflected in the pattern of ozone (Fig. 6, bottom), which is simulated to reach a minimum of 47 ppb_v at an initial IOA

concentration of 50 μg/m^3. Above this IOA concentration ozone increases similarly reaching 52 ppb$_v$ at IOA = 150 μg/m^3 for the simulated conditions in Los Angeles. The impact of IOA at these conditions is therefore notable but moderate.

With respect to SOA formed in the vicinity from the gas-phase and thus explicitly calculated in the model the most important compounds were BVOCs with high molar masses, a substantial degree of oxidation and thus lowest saturation vapour pressures that were formed to a notable extend. For the Los Angeles conditions those were primarily organic nitrates followed by some acids and hydroperoxides representing derivatives of both pinenes used as surrogates for the monoterpenes present. Anthropogenic SOA (ASOA) was formed too. The contribution of oxygenated aromatic species and derivatives was highest, with organic nitrates in the lead. But total sum of ASOA was calculated negligible for the situation studied because of the smaller molecules and the corresponding higher saturation vapour pressures. This may change for different locations as the contribution of local ASOA and BSOA species refers to the source intensity of traffic, industry, household as well as vegetation abundance and species composition in the vicinity and the oxidation strength enhancing the formation process.

3.4 Contributions of individual VOCs and OA: anthropogenic and biogenic

Having addressed the individual effects separately we concentrate on Berlin at summer at the time of most intense ozone production (maximum approach) during the BAERLIN2014 campaign.

Berlin is a megacity with about 3.5 million inhabitants, several industries and a large vegetated area (33% by area, Berlin Senate, 2010) as well as intensive street traffic and is surrounded by large motorways with remarkable transport from West to East and North to South and vice versa. Urban traffic supplies large amounts of NO_x and VOCs. Therefore, ozone production in the German capitol is affected by most of the VOC groups (Fig. 7). Isoprene (BVOC), aromatics and alkanes provided the largest contributions closely followed by IOA. Carbonyl compounds contributed only to a minor extend. The large vegetative area (>30%) is apparent by the remarkable reductive effects for monoterpenes and the related SOA mass formed. Both compensate effects of smaller and more volatile organic trace gases. Consequently, the budget for the biogenic VOC impact on urban ozone in Berlin is reductive in total although the largest ozone forcing pollutant is isoprene. An important result of Figure 7 is the current outweigh of isoprene and monoterpene effects resulting in a small ozone effect of the total vegetation. However this is emission dependent and clearly indicates that the importance of vegetation emission as a key aspect for ozone in Berlin and future developments.

3.5 Effect of different vegetation types on processes strength and air pollution

This key aspect of vegetation was investigated by assessing different vegetation types present or potential future ones via BVOC emissions, ozone production or destruction, SOA and OH creation. While the filtering effect of particulate masses such as described by Tiwary et al. (2009) is potentially of high importance, it cannot be separated from local meteorological conditions, ventilation (e.g. building arrangements) and vegetation properties such as size, age and development stage. For a spatially explicit approach that might be needed for future urban planning, the incorporation of this effect is recommended.

Global radiation fluxes at Berlin are medium and can reach up to 1000 W m^{-2}, which is about twice the available PAR. To demonstrate the effect of different tree types and emissions on ozone in Berlin we have chosen (a) a strong isoprene emitter (plane), (b) an emitter of isoprene and monoterpenes (American sweetgum) and (c) a strong monoterpene emitter (magnolia). Plane trees, which are common species in Central Europe, cause ozone to increase by +31% (from 90.4 to 119.7 ppb_v, Table S3) for typical summer conditions at 35°C. A sole contribution of monoterpene emitting species reduce ozone at identical conditions by -2% (from 90.4 to 89.9 ppb_v, Table S3). To make this evident the ozone volume mixing ratios are plotted in Fig. 8 as a function of time (horizontal axis) and of additional vegetation area by plane, American sweetgum or magnolia compared to the vegetation emissions estimated to fit ozone mixing ratios to observations. The "fitted standard" vegetation emission was treated as *Carpinus betula* ($E_{isop,0}$ = 0.1 μg/g(dw)/h, $E_{MT,0}$ = 0.04 μg/g(dw)/h). In this way '10%' indicates 28.1 km^2 additional vegetation area or comparable amount of trees planted in the urban landscape (green spaces in Berlin: 280.5 km^2, http://www.stadtentwicklung.berlin.de/umwelt/stadtgruen/gruenanlagen/de/daten_fakten/downloads/ausw_5.pdf). It is apparent that increasing vegetation using plane trees increases the isoprene and thus the ozone volume mixing ratio substantially, while adding magnolia trees reduces ozone but enhances SOA and thus PM10 production. American sweetgum trees however, seem to be in line with the currently compensating effect of isoprene and monoterpene emissions and increasing their contribution will hardly cause notable changes with respect to the pollutants.

A second investigation was done exchanging the best fit vegetation by a series of urban or typical German trees as potential candidates for urban greening in Germany. This investigation was focussed on ozone production, concentration, SOA (PM_{10}) production and concentration and OH concentrations for different temperatures and temperature related changes for example under potential future climate conditions (Tables S3-S5). Therefore, identical simulations (temperature, VOCs except BVOCs, PM_{10}, MLH and radiation) were conducted with different BVOC emissions for a large number of tree species. In order to study temperature related changes a series of runs was performed for each tree species for a range of temperatures ($T+\Delta T$ with ΔT = +0, +2, +4, +6, +8, +10 and +14 K). This was fitted twice, (a) with a polynomial fit of 3rd order and (b) with a linear fit for the lower temperature runs ($+0K \leq \Delta T \leq +10$ K). Several characteristics are displayed in Tables S3-S5. While ozone production rate ($P(O_3)$) is identical for the reference simulation and the corresponding one without BVOCs, the ozone volume mixing ratio is gently smaller. This indicates an intensified ozone sink in the presence of BVOCs, i.e. alkene-ozone reactions. With respect to the different tree species the ozone volume mixing ratio and $P(O_3)$ behaviour reflects the individual isoprene and monoterpene emission strength (Fig. 9, left): The higher the isoprene emission the more intense the ozone production (Fig. 9, centre) and as a follow up the ozone mixing ratio. Thus the highest increase in $P(O_3)$ is with red oak ($P(O_3)$ = 40.5 ppb/h, isoprene standard emission at T = 30°C $E_{isop,0}$ = 100 μg/g(dw)/h), tupelo ($P(O_3)$ = 35.7 ppb/h, $E_{isop,0}$ = 75 μg/g(dw)/h) and other oak species ($P(O_3)$ = 31 ppb/h, $E_{isop,0}$ = 62.8 μg/g(dw)/h), followed by a series of deciduous trees. On the contrary, monoterpene emissions like magnolia ($P(O_3)$ = 10.5 ppb/h, monoterpene standard emission rate at T = 30°C $E_{MT,0}$ = 57 μg/g(dw)/h), beech ($P(O_3)$ = 11.4 ppb/h, $E_{MT,0}$ = 43.5 μg/g(dw)/h) and wayfaring trees ($P(O_3)$ = 10.9 ppb/h, $E_{MT,0}$ = 100 μg/g(dw)/h) tend to lower the ozone production rate by up to 7% at 35°C . Please note the different effect of temperature caused by different emission characteristics, i.e. temperature and for some species PAR dependencies. This can be parameterised for Berlin conditions as

(2) $\Delta P(O_3) = (0.161 \pm 0.005)\ ppb*g(dw)/\mu g*E_{isop}(T) - (0.012 \pm 0.008)\ ppb*g(dw)/\mu g*E_{MT}(T)$

as presented in Fig. 9 at the bottom ($R^2 = 0.98$) for T = 35°C. The temperature dependency causes some of the tree species emissions to act more reductive at warmer conditions (not shown). Especially the conifers represent rising monoterpene emissions and cause significant effects above 40°C. Ozone volume mixing ratio effects behave quite similar to $P(O_3)$, although the emissions of common beech indicate a stronger reduction effect based on the additive ozone sink reaction with monoterpenes.

(3) $\Delta O_3 = (0.308 \pm 0.010)\ ppb*h*g(dw)/\mu g*E_{isop}(T) - (0.017 \pm 0.017)\ ppb*h*g(dw)/\mu g*E_{MT}(T)$

The simulations indicate that below 35°C the effect of monoterpene emissions is insignificant. This is partially triggered by different emission characteristics (on- and offline) and their dependency on temperature. But the monoterpene effect evolves with increasing temperature and offline emission contributions, when temperature becomes the primary emission controlling factor. Beech emissions act moderately reductive on ozone due to its strong effect as ozone sink increasing with temperature already at ca. 35°C. This behaviour can be observed for most monoterpene emitting species above 40°C, while species that are well-known for high isoprene emissions (e.g. black locust, different oak oak species, plane trees, poplars, tupelo and willows) don't show this behaviour (see also Drewniak et al., 2014).

With respect to OH, our cleansing agent of the atmosphere, several characteristics seen for $P(O_3)$ and ozone maintain, such as the highest ozone effects are reflected in OH concentrations (isoprene emitter: black locust, oak, plane, poplar, red oak, tupelo and willow): between +39 and +83% at 35°C). Several reducing tree species appear with high monoterpene emission rates.

(4) $\Delta OH = (8.71 \pm 0.38) \times 10^4\ cm^{-3}*h*g(dw)/\mu g*E_{isop}(T) - (1.61 \pm 0.68) \times 10^4\ cm^{-3}*h*g(dw)/\mu g*E_{MT}(T)$

Highest reduction effects occur for magnolia and wayfaring tree emissions, -12% respectively, followed by beech, chestnut, Douglas fir and laurel cause reductions between 6 and 7%. These are closely followed by a group of conifers and birch emissions with a tendency but not significant changes at 35°C. Their effects pile up as temperature increases. Other tree species with minor emissions do not show significant contributions in the considered temperature range.

With respect to aerosol particle number concentration PNC, most particles seem to have formed by traffic exhaust, which cooled down rapidly by the end of the cars pipe and may have formed by different processes (correlation coefficients: PNC+NO_2 = 0.68, PNC+CO = 0.55, PNC+benzene = 0.48, PNC+NO = 0.43, PNC+toluene = 0.42, PNC+global radiation = 0.13, PNC+SO_2 = 0.02). No clear estimate for an effect of a changing vegetation is possible.

The totally formed secondary organic aerosol mass displays similar dependencies on BVOC emissions as OH:

(5) $\Delta SOA = (0.0052 \pm 0.0002)*h*g(dw)/m^3*E_{isop}(T) - (0.028 \pm 0.002)*h*g(dw)/m^3*E_{MT}(T)$

Equation 5 accentuates the higher (negative) impact of monoterpenes on SOA formation than of isoprene emissions (positive). This effect is predominantly originating in the higher capability of monoterpene oxidation products to form SOA mass and in the oxidation of VOCs by OH and thus serving more oxidation groups and lowering the saturation vapour pressure. Please note that for the

selected urban conditions, BVOCs are still less important than anthropogenic VOCs. The latter are primarily oxidized by OH. Although partially emitted as rapidly condensed droplets by traffic, the box model assumes that most of these compounds may evaporate afterwards (i.e. reestablish equilibrium between gas-phase and aerosol-phase) before being oxidized and entering the aerosol-phase again.

While the different tree species display a series of positive and negative effects on urban air quality, to which actually the filtering effect of urban trees add up, the aspect of urban greening depends essentially on two further aspects, i.e. (i) price for planting and maintenance and (ii) sensitivity of areas with respect to pollutants (local burden, health issues and chemical conditions).

3.6 Implications for future urban vegetation management: Economy vs. sensitivity and pollution

Primary goal of urban trees plantings in some countries in 19th century have been to provide a public open space for health and recreation (Pincetl al., 2012). Biogenic VOC emissions from urban trees have not been taken into account in selecting urban tree species. Changing current composition of tree species towards decreasing their VOC emissions and respective ozone mixing ratio, e.g., by replacing *Q. Rubra* and *Poplus spp* by *Magnolia grandifolia* and *Fagus Sylvatica* becomes crucial in highly polluted mega cities.

However, as the current replanting and maintenance cost per tree is relatively high (ca. 1350 €, www.stadtentwicklung.berlin.de/umwelt/stadtgruen/stadtbaeume/kampagne/de/faq/index.shtml, access: 29.5.2017), the action may become highly costly to realize at a time and asks for a sustainable conversion of urban tree species composition over time. The conversion strategy should be not only cost-effective, but also incorporate other ecosystem services and values and consider adaptability of tree species to future climate conditions. For this, urban forestry may borrow already developed approaches in forestry, e.g. simulation-optimization for a multi-purpose forest conversion (Yousefpour et al., 2009), to increase cost-efficiency of conversions.

4 Conclusions

In this study we have presented an extended version of the MECCA box model including the set-up of measured boundary conditions, their evolution with time, the treatment of different secondary organic aerosol sources and approaches as well as online biogenic VOC emission calculations. The model set-up allowed investigation of the effect of modified vegetation characteristics with respect to BVOC exchange. Since estimations of the effective area of e.g. BVOC emissions or transport of pollutants for ozone production and lifetime results in an area of 40 km in distance at maximum, an integration/averaging of substantial areas is required to make reasonable calculations and predictictions. This task can be addressed reasonably well with a box model driven by local observations such as meteorology, gaseous concentrations and vegetation properties.

With respect to the area of Berlin we found substantial contributions of alkenes, aromatics and isoprene to ozone formation, while monoterpenes and SOA contributions were calculated as reductive. Magnitudes of specific compounds were found to depend on conditions such as emission and radiation intensity, vertical dilution and temperature. This confirms our hypothesis on the different impacts of tree species in cities. Urban SOA effects had opposite effects during day and night. During night-time, NO_x species were converted to organic nitrates that partially were absorbed

into the available organic particulate matter and the ozone sink decreased (ozone increase). During day-time the locally formed SOA removed more oxygenated VOCs than during the night and decreased the total ozone production rate by the slower reaction of VOCs with OH. The initially available OA was relevant for ozone formation to a substantial extend (ca. 40% of total OA effect), while we found locally produced SOA to dominate the process (ca. 60% of total OA effect). IOA contributed extra VOCs, desorbing from the particles and joining the ozone production cycle, SOA removed VOCs from the ozone production cycle, causing opposite effects to ozone concentrations. Essentially both processes are needed for accurately predictions.

As a consequence future climate warming and urban greening have the potential to significantly alter tropospheric ozone production (intensification or weakening). Depending on the choice of tree and thus biogenic emission types, the calculated effects may result in several ppb_v per hour change in ozone production (up to a doubling at worst), in OH and in SOA concentrations compared to the current levels at 30°C. In order to minimize potential ozone and particulate enhancement because of vegetation, we recommend choosing less stress sensitive tree types with reduced BVOC emissions and resulting SOA mass production but similar CO_2 and water exchange. This would allow plant "filtering" effects, which are expected to cause significant particle mass reduction effects (perhaps >10% during passage over Berlin) including changes in regional PM_{10} chemical composition to locally formed species. The expected reduction in particle mass and surface area will cause enhanced new particle number formation, which will be minor compared to the one caused by traffic, industrial processes and heating related particle formation rates. Finally, we conclude that any of the three added processes, i.e. MLH development, biogenic VOC emissions and organic aerosols is essential for addressing urban ozone formation and its future development.

Acknowledgements

This work was done primarily at the Institute of Advanced Sustainability Studies (IASS) in Potsdam, Germany and was funded by the Federal and Brandenburg Ministries (BMBF and MWFK). Thanks for the financial support and engagement of all the numerous co-workers without whom this study would have been impossible. Christoph Münkel, Vaisala GmbH, Hamburg should be thanked for his important support during measurement and analysis. Thanks very much to the CARES and CalNex participants for sharing their data and to Klaus Müller (Free University of Berlin, Germany) for providing the meteorological data from the Botanical Garden allowing a basic radiation correction. Special thanks to all BAERLIN2014 partners for excellent cooperation, sharing the data and making this study possible.

References

Affolderbach, J., and Schulz, C., 2017. Positioning Vancouver through urban sustainability strategies? The Greenest City 2020 Action Plan. J. Clean. Prod., 164, 676-685, doi: 10.1016/j.jclepro.2017.06.234.

Atkinson, R., Baulch, D. L., Cox, R. A., Crowley, J. N., Hampson, R. F., Hynes, R. G., Jenkin, M. E., Rossi, M. J., Troe, J., and IUPAC Subcommittee, 2006. Evaluated kinetic and photochemical data for atmospheric chemistry: Volume II – gas phase reactions of organic species. Atmos. Chem. Phys., 6, 3625-4055, doi: 10.5194/acp-6-3625-2006.

Berlin Senate, 2010. Flächennutzung und Stadtstruktur, Senatsverwaltung für Stadtentwicklung, Berlin.

Bloss, C., Wagner, V., Jenkin, M.E., Volkamer, R., Bloss, W.J., Lee, J.D., Heard, D.E., Wirtz, K., Martin-Reviejo, M., Rea, G., Wenger, J.C., and Pilling, M.J., 2005. Development of a detailed chemical mechanism (MCMv3.1) for the atmospheric oxidation of aromatic hydrocarbons. Atmos. Chem. Phys., 5, 641-664, doi: 10.5194/acp-5-641-2005.

Bonn, B., von Schneidemesser, E., Andrich, D., Quedenau., J., Gerwig, H., Lüdecke, A., Kura, J., Pietsch, A., Ehlers, C., Klemp, D., Kofahl, C., Nothard, R., Kerschbaumer, A., Junkermann, W., Grote, R., Pohl, T., Weber, K., Lode, B., Schönberger, P., Churkina, G., Butler, T.M., and Lawrence, M.G., 2016. BAERLIN2014 – the influence of land surface types on and the horizontal heterogeneity of air pollutant levels in Berlin. Atmos. Chem. Phys., 16, 7785-7811, doi: 10.5194/acp-16-7785-2016.

Butler, T.M., Lawrence, M.G., Taraborrelli, D., and Lelieveld, J., 2011. Multi-day ozone production potential of volatile organic compounds calculated with a tagging approach. Atmos. Environ., 45, 4082-4090, doi: 10.1016/j.atmosenv.2011.03.040.

Calfapietra, C., Fares, S., Manes F., Morani, A., Sgrigna, G., and Loreto F., 2013. Role of Biogenic Volatile Organic Compounds (BVOC) emitted by urban trees on ozone concentration in cities: A review. Environ. Poll., 183, 71-80, doi: 10.1016/j.envpol.2013.03.012

Churkina, G., Grote, R., Butler, T. M., and Lawrence, M., 2015. Natural selection? Picking the right trees for urban greening. Environ. Sci. Policy, 47, 12-17, doi: 10.1016/j.envsci.2014.10.014.

Churkina, G., Kuik, F., Bonn, B., Lauer, A., Grote, R., Tomiak, K., and Butler, T., 2017. Effect of VOC emissions from vegetation on air quality in Berlin during a heatwave. Environ. Sci. Technol., accepted, doi: 10.1021/acs.est.6b065.

Chuwah, C., van Noije, T., van Vuuren, D.P., Stehfest, E., and Hazeleger, W., 2015. Global impacts of surface ozone changes on crop yields and land use. Atmos. Environ., 106, 11-23, doi: 10.1016/j.atmosenv.2015.01.062.

Donahue, N.M., Robinson, A.L., Stanier, C.O., and Pandis, S.N., 2006. Coupled partitioning, dilution, and chemical ageing of semivolatile organics. Environ. Sci. Technol., 40, 2635-2643, doi: 10.1021/es052297c.

Drewniak, B.A., Snyder, P.K., Steiner, A.L., Twine, T.E., and Wuebbles, D.J., 2014. Simulated changes in biogenic VOC emissions and ozone formation from habitat expansion of Acer Rubrum (red maple). Environ. Res. Lett., 9, 014006 (10pp), doi:10.1088/1748-9326/9/1/014006.

Ehlers, C., Klemp, D., Rohrer, F., Wahner, A., Dörksen, H., Simon, S., Menger, L., and Strey, R., 2013. Formation of “white soot” by diesel cars equipped with particle filters. Extended abstract, 17th Conference on Combustion related Particles, Zurich, Switzerland.

Ehlers, C., 2014. Mobile Messungen – Messung und Bewertung von Verkehrsemissionen, PhD thesis, Cologne University, Cologne, Germany, 136 p, ISBN: 978-3-89336-989-8.

Faiola, C. L., Jobson, B. T., and VanReken, T. M., 2015. Impacts of simulated herbivory on volatile organic compound emission profiles from coniferous plants. Biogeosciences, 12, 527–547, doi: 10.5194/bg-12-527-2015.

Fares, S., Vargas, R., Detto, M., Goldstein, A.H., Karlik, J., Paoletti, E., and Vitale, M., 2013. Tropospheric ozone reduces carbon assimilation in trees: Estimates from analysis of continuous flux measurements. Global Change Biol., 19, 2427-2443, doi: 10.1111/gcb.12222.

Fu, Y., and Liao, H., 2014. Impacts of land use and land cover changes on biogenic emissions of volatile organic compounds in China from the late 1980s to the mid-2000s: implications for tropospheric ozone and secondary organic aerosol. Tellus B, 66, 24987, doi:10.3402/tellusb.v66.24987

Geiß, A., Wiegner, M., Bonn, B., Schäfer, K., Forkel, R., von Schneidemesser, E., Münkel, C., Chan, K.L., and Nothard, R., 2017. Mixing layer height as an indicator for urban air quality? Atmos. Meas. Tech., 10, 2969-2988, doi: 10.5194/amt-10-2969-2017.

Ghirardo, A., Xie, J., Zheng, X., Wang, Y., Grote, R., Block, K., Wildt, J., Mentel, T., Kiendler-Scharr, A., Hallquist, M., Butterbach-Bahl, K., and Schnitzler, J.-P., 2016. Urban stress-induced biogenic VOC emissions impact secondary aerosol formation in Beijing. 16, 2901-2920, doi: 10.5194/acp-16-2901-2016.

Goldstein, A. H., and Galbally, I. E., 2007. Known and unexplored organic constituents in the Earth's atmosphere. Environ. Sci. Technol., 41, 1514–1521, doi: 10.1021/es072476p.

Guenther, A., Hewitt, C.N., Erickson, D., Fall, R., Geron, C., Graedel, T., Harley, P., Klinger, L., Lerdau, M., McKay, W.A., Pierces, T., Scholes, B., Steinbrecher, R., Tallamraju, R., Taylor, J., and Zimmerman, P., 1995. A global model of natural volatile organic compound emissions. J. Geophys. Res., 100, 8873-8892, doi: 10.1029/94JD02950.

Guenther, A., Karl, T., Harley, P., Wiedinmyer, C., Palmer, P. I., and Geron, C., 2006. Estimates of global terrestrial isoprene emissions using MEGAN (Model of Emissions of Gases and Aerosols from Nature). Atmos. Chem. Phys., 6, 7551–7575, doi:10.5194/acp-7-7551-2006.

Isaacman, G., Worton, D. R., Kreisberg, N. M., Hennigan, C. J., Teng, A. P., Hering, S. V., Robinson, A. L., Donahue, N. M., and Goldstein, A. H., 2011. Understanding evolution of product composition and volatility distribution through in-situ GC×GC analysis: a case study of longifolene ozonolysis. Atmos. Chem. Phys., 11, 5335–5346, doi: 10.5194/acp-11-5335-2011.

Jenkin, M.E., Saunders, S.M., and Pilling, M.J., 1997. The tropospheric degradation of volatile organic compounds: A protocol for mechanism development. Atmos. Environ., 31, 81-104, doi: 10.1016/S1352-2310(96)00105-7.

Jenkin, M.E., Saunders, S.M., Wagner, V., and Pilling, M.J., 2003. Protocol for the development of the Master Chemical Mechanism, MCM v3 (Part B): Tropospheric degradation of aromatic volatile organic compounds. Atmos. Chem. Phys., 3, 181-193, doi: 10.5194/acp-3-181-2003.

Jimenez, J.L., Canagaratna, M. R., Donahue, N. M., Prevot, A. S. H., Zhang, Q., Kroll, J. H., DeCarlo, P. F., Allan, J. D., Coe, H., Ng, N. L., Aiken, A. C., Docherty, K. S., Ulbrich, I. M., Grieshop, A. P., Robinson, A. L., Duplissy, J., Smith, J. D., Wilson, K. R., Lanz, V. A., Hueglin, C., Sun, Y. L., Tian, J., Laaksonen, A.,

Raatikainen, T., Rautiainen, J., Vaattovaara, P., Ehn, M., Kulmala, M., Tomlinson, J. M., Collins, D. R., Cubison, M. J., Dunlea, J., Huffman, J. A., Onasch, T. B., Alfarra, M. R., Williams, P. I., Bower, K., Kondo, Y., Schneider, J., Drewnick, F., Borrmann, S., Weimer, S., Demerjian, K., Salcedo, D., Cottrell, L., Griffin, R., Takami, A., Miyoshi, T., Hatakeyama, S., Shimono, A., Sun, J. Y., Zhang, Y. M., Dzepina, K., Kimmel, J. R., Sueper, D., Jayne, J. T., Herndon, S. C., Trimborn, A. M., Williams, L. R., Wood, E. C., Middlebrook, A. M., Kolb, C. E., Baltensperger, U., and Worsnop, D. R., 2008. Evolution of Organic Aerosols in the Atmosphere. Science, 26, 1525-1529, doi: 10.1126/science.1180353.

Jud, W., Fischer, L., Canaval, E., Wohlfahrt, G., Tissier, A., and Hansel, A., 2016a. Plant surface reactions: an ozone defence mechanism impacting atmospheric chemistry. Atmos. Chem. Phys., 16, 277-292, doi: 10.5194/acp-16-277-2016.

Jud, W., Vanzo, E., Li, Z., Ghirardo, A., Zimmer, I., Sharkey, T.D., Hansel, A., and Schnitzler, J.-P., 2016b. Effects of heat and drought stress on post illumination bursts of volatile organic compounds in isoprene emitting and non-emitting poplar. Plant Cell Environ., 39, 1204–1215, doi: 10.1111/pce.12643.

Karlik, J.F., and Pittenger, D.R., 2016. Biogenic hydrocarbon emissions: a consideration for large-scale tree planting programs. Acta Hortic., 1108, 255-262, in Proc. Int. Conf. on Landscape and Urban Horticulture and International Symposium on Sustainable Management in the Urban Forest (ed. G. Groening et al.), doi: 10.17660/ActaHortic.2016.1108.33

Kofahl, C., 2012. Hochempfindliche Bestimmung der organischen und anorganischen Kohlenstoff-Fraktion in Feinstaubproben mittels CRD-Spektroskopie, University of Applied Sciences, Aachen, Campus Jülich, Jülich, Germany.

Leal Filho, W., Icaza, L. E., Neht, A., Klavins, M., and Morgan, E. A., 2018. Coping with the impacts of urban heat islands. A literature based study on understanding urban heat vulnerability and the need for resilience in cities in a global climate change context. J. Clean. Prod., 171, 1140-1149, doi: 10.1016/j.jclepro.2017.10.086.

Lelieveld, J., Evans, J. S., Fnais, M., Giannadaki, D., and Pozzer, A., 2015. The contribution of outdoor air pollution sources to premature mortality on a global scale. Nature, 525, 367-371, doi: 10.1038/nature15371.

Liu, H., Hu, Y., Li, F., and Yuan, L., 2018. Associations of multiple ecosystem services and disservices of urban park ecological infrastructure and the linkages with socioeconomic factors. J. Clean. Prod., 174, 868-879, doi: 10.1016/j.jclepro.2017.10.139.

Loreto, F., and Velikova, V., 2001. Isoprene produced by leaves protects the photosynthetic apparatus against ozone damage, quenches ozone products and reproduces lipid peroxidation of cellular membranes. Plant Physiol., 127, 1781-1787, doi: 10.1104/pp.010497.

Loreto, F., Pollastri, S., Fineschi, S., and Velikova, V., 2014. Volatile isoprenoids and their importance for protection against environmental constraints in the Mediterranean area. Environ. Experimental Botany, 103, 99-106, doi: 10.1016/j.envexpbot.2013.09.005.

Maroušek, J., Vochozka, M., Plachý, J., and Žák, J., 2017. Glory and misery of biochar. Clean Technol. Enir., 19, 311–317, doi: 10.1007/s10098-016-1284-y.

McPherson, E.G., Simpson, J.R., Xiao, Q., and Wu, C., 2011. Million trees Los Angeles canopy cover and benefit assessment. Landscape Urban Plan., 99, 40-50, doi: 10.1016/j.landurbplan.2010.08.011.

Pankow, J.F., 1994a. An absorption model of gas/particle partitioning of organic compounds in the atmosphere. Atmos. Environ. 28, 185-188, doi: 10.1016/1352-2310(94)90093-0.

Pankow, J.F., 1994b. An absorption-model of the gas aerosol partitioning involved in the formation of secondary organic aerosol. Atmos. Environ. 28, 189-193, doi: 10.1016/1352-2310(94)90094-9.

Parrish, D.D., 2014. CalNex 2010 Synthesis: Final Report, Synthesis of Policy Relevant Findings from the CalNex 2010 Field Study (California Research at the Nexus of Air Quality and Climate Change), Final Report to the Research Division of the California Air Resources Board, ARB Agreement No. 10-326, 210 p., Boulder, CO, USA.

Pope III, C.A., Ezzati, M., and Dockery, D.W., 2009. Fine-particulate air pollution and life expectancy in the United States. New Engl. J. Med., 360, 376-386, doi: 10.1056/NEJMsa0805646.

Pincetl, S., Bunje, P., and Holmes, T., 2012. An expanded urban metabolism method: Toward a systems approach for assessing urban energy processes and causes. Landscape Urban Plan., 107, 193-202, doi: 10.1016/j.landurbplan.2012.06.006.

Sander, R., Baumgaertner, A., Gromov, S., Harder, H., Jöckel, P., Kerkweg, A., Kubistin, D., Regelin, E., Riede, H., Sandu, A., Taraborrelli, D., Tost, H., and Xie, Z.-Q., 2011. The atmospheric chemistry box model CAABA/MECCA-3.0. Geosci. Model Dev., 4, 373–380, doi:10.5194/gmd-4-373-2011.

Sandu, A., and Sander, R., 2006. Technical note: Simulating chemical systems in Fortran90 and Matlab with the Kinetic PreProcessor KPP-2.1. Atmos. Chem. Phys., 6, 187-195, doi:10.5194/acp-6-187-2006.

Saunders, S.M., Jenkin, M.E., Derwent, R.G., and Pilling, M.J., 2003. Protocol for the development of the Master Chemical Mechanism, MCM v3 (Part A): Tropospheric degradation of non-aromatic volatile organic compounds. Atmos. Chem. Phys., 3, 161-180, doi:10.5194/acp-3-161-2003.

Seinfeld, J.H., and Pandis, S.N., 2006. Atmospheric chemistry and physics: From air pollution to climate change. 2nd ed., Wiley Interscience, Oxford.

Stein, S.E., and Brown, R.L., 1994. Estimation of normal boiling points from group contributions. J. Chem. Inf. Comp. Sci., 34, 581-587, doi: 10.1021/ci00019a016.

Tiwary, A., Sinnett, D., Peachey, C., Chalabi, Z., Vardoulakis, S. Fletcher, T., Leonardi, G., Grundy, C., Azapagic, A., and Hutchings, T.R., 2009. In integrated tool to assess the role of new planting in PM_{10} capture and the human health benefits: A case study in London. Environ. Poll., 157, 2645-2653, doi: 10.1016/j.envpol.2009.05.005

Tiwary, A., Namdeo, A., Fuentes, J., Dore, A., Hu, X.-M., Bell, M., 2013. Systems scale assessment of the sustainability implications of emerging green initiatives. Environ. Poll., 183, 213-223, doi: 10.1016/j.envpol.2013.03.049.

von Schneidemesser, E. , Bonn, B., Butler, T. M., Ehlers, C., Gerwig, H., Hakola, H., Hellén, H., Kerschbaumer, A., Klemp, D., Kofahl, C., Kura, J., Lawrence, M. G., Lüdecke, A., Nothard, R., Pietsch,

A., Schaefer, K., Schauer, J.J., Villalobos, A.M., 2017. BAERLIN2014 – stationary measurements and source apportionment at an urban background station in Berlin, Germany. Atmos. Chem. Phys. Diss., in review, 37p., doi: 10.5194/acp-2017-1049.

Winkler, J., Blank, P., Glaser, K., Gomes, J.A.G., Habram, M., Jambert, C., Jaeschke, W., Konrad, S., Kurtenbach, R., Lenschow, P., Lörzer, J.C., Perros, P.E., Pesch, M., Prümke, H.J., Rappenglück, B., Schmitz, Th., Slemr, F., Volz-Thomas, A., and Wickert, B., 2002. Ground-Based and Airborne Measurements of Nonmethane Hydrocarbons in BERLIOZ: Analysis and Selected Results. J. Atmos. Chem., 42, 465–492, doi: 10.1023/A:1015709214016.

Yousefpour, R., 2009. Adaptation to Climate Change within Multi-purpose Forest Management Using Hybrid Simulation Optimization Models. PhD thesis, University of Freiburg, Germany, 180 p.

Table 1.

Novel compounds considered in approach A1. Gaseous compounds of anthropogenic (first letter 'C' for the gas-phase, middle letter is 'A' as e.g. CAS) and biogenic (middle letter is 'B' e.g. CBS) species are considered as precursors. Other types derive from oxidation. All compounds have corresponding compounds in the particle phase starting with 'A' like 'aerosol particle' instead of 'C'.

compound	*Description, p_{sat} in Pa*	*compound*	*description*	*compound*	*description*
CAS1	anthr. species, $10^{-2} < p_{sat} < 1$	CP09	peroxides, $10^{6} < p_{sat} < 10^{7}$	CH05	hydroperoxides, $100 < p_{sat} < 10^{3}$
CAS2	anthr. species, $1 < p_{sat} < 100$	CP010	peroxides, $p_{sat} > 10^{7}$	CH06	hydroperoxides, $10^{3} < p_{sat} < 10^{4}$
CAS3	anthr. species, $100 < p_{sat} < 10^{4}$	CO01	multi. ox. org., $10^{-2} < p_{sat} < 10^{-1}$	CH07	hydroperoxides, $10^{4} < p_{sat} < 10^{5}$
CAS4	anthr. species, $10^{4} < p_{sat} < 10^{6}$	CO02	multi. ox. org, $10^{-1} < p_{sat} < 1$	CH08	hydroperoxides, $10^{5} < p_{sat} < 10^{6}$
CBS1	biog. species, $10^{-2} < p_{sat} < 1$	CO03	multi. ox. org, $1 < p_{sat} < 10$	CH09	hydroperoxides, $10^{6} < p_{sat} < 10^{7}$
CBS2	biog. species, $1 < p_{sat} < 100$	CO04	multi. ox. org, $10 < p_{sat} < 100$	CH010	hydroperoxides, $p_{sat} > 10^{7}$
CBS3	biog. species, $100 < p_{sat} < 10^{4}$	CO05	multi. ox. org, $100 < p_{sat} < 10^{3}$	CN01	org. nitrates, $10^{-2} < p_{sat} < 10^{-1}$
CBS4	biog. species, $10^{4} < p_{sat} < 10^{6}$	CO06	multi. ox. org, $10^{3} < p_{sat} < 10^{4}$	CN02	org. nitrates, $10^{-1} < p_{sat} < 1$
CP01	peroxides, $10^{-2} < p_{sat} < 10^{-1}$	CO07	multi. ox. org, $10^{4} < p_{sat} < 10^{5}$	CN03	org. nitrates, $1 < p_{sat} < 10$
CP02	peroxides, $10^{-1} < p_{sat} < 1$	CO08	multi. ox. org, $10^{5} < p_{sat} < 10^{6}$	CN04	org. nitrates, $10 < p_{sat} < 100$
CP03	peroxides, $1 < p_{sat} < 10$	CO09	multi. ox. org, $10^{6} < p_{sat} < 10^{7}$	CN05	org. nitrates, $100 < p_{sat} < 10^{3}$
CP04	peroxides, $10 < p_{sat} < 100$	CO010	multi. ox. org, $p_{sat} > 10^{7}$	CN06	org. nitrates, $10^{3} < p_{sat} < 10^{4}$
CP05	peroxides, $100 < p_{sat} < 10^{3}$	CH01	hydroperoxides, $10^{-2} < p_{sat} < 10^{-1}$	CN07	org. nitrates, $10^{4} < p_{sat} < 10^{5}$
CP06	peroxides, $10^{3} < p_{sat} < 10^{4}$	CH02	hydroperoxides, $10^{-1} < p_{sat} < 1$	CN08	org. nitrates, $10^{5} < p_{sat} < 10^{6}$
CP07	peroxides, $10^{4} < p_{sat} < 10^{5}$	CH03	hydroperoxides, $1 < p_{sat} < 10$	CN09	org. nitrates, $10^{6} < p_{sat} < 10^{7}$
CP08	peroxides, $10^{5} < p_{sat} < 10^{6}$	CH04	hydroperoxides, $10 < p_{sat} < 100$	CN010	org. nitrates, $p_{sat} > 10^{7}$

Table 2.

Chemical gas-phase reactions of an exemplary novel compound considered for A1. A complete list of all reactions and reaction rate constants can be found in the appendix (Table S2).

$X_n + OH\ (+O_2)$	$\rightarrow$	$X_nO2\ (+H_2O)$	
$X_nO2 + HO2$	$\rightarrow$	X_{n-1}	
$X_nO2 + NO$	$\rightarrow$	X_{n-1}	(50%)
$X_nO2 + NO$	$\rightarrow$	$X_nO + NO_2$	(50%)
$X_nO2 + RO_2$	$\rightarrow$	X_{n-1}	(40%)
$X_nO2 + RO_2$	$\rightarrow$	$X_nO\ (+O_2) + RO$	(60%)
X_nO	$\rightarrow$	$X_{n-1} + HO_2$	

Table 3.

List of nine VBS sections, the corresponding saturation concentration $c_{sat,0}$ ranges, related typical compound classes, dominant compound surrogates associated with the individual volatility bins, their molar masses M_w, chemical gas-phase reaction rates k_X and enthalpy changes Δh between gas- and particle phase for approach A2. If two compounds are named, they are assumed to be abundant equal (50%:50%). For names and photolysis rates see Jenkin et al. (1997; 2003) and Saunders et al.(2003).

VBS box no.	*$c_{sat,0}$ [$\mu g/m^3$]*	*compound class*	*MCM surrogate*	*M_w [g/mol]*	*k [$cm^3\ s^{-1}$], J [s^{-1}]*	*Δh [kJ/mol]*
9	$>10^6$	alkanes, alkenes, aromatics	toluene (, NC6H14)	92±20	$k_{OH} = (4.7\pm3.6)x10^{-12}$	33±3
8	10^5-10^6	carbonyl compounds	MALDIAL (50%), TLFUONE(50%)	92±30	$k_{OH} = (6.1\pm1.4)x10^{-11}$ $k_{NO3}=10^{-13}$ $k_{O3} = 1.4x10^{-18}$	37±5
7	10^4-10^5	org. nitrates, smaller alcohols	TLIPERNO3	171±40	$k_{OH} = (7.2\pm3.5)x10^{-11}$ J_{54} (MCMv3.2)	38±5
6	10^3-10^4	alcohols	CRESOL	108±20	$k_{OH} = (6\pm2)x10^{-11}$ $k_{NO3} = (1.4\pm0.5)x10^{-11}$	50±2
5	10^2-10^3	hydroperoxides, monocarb. acids	TLBIPEROOH, C5CO14OH	142±30	$k_{OH} = (2.4\pm1.6)x10^{-11}$ J_{41} (MCMv3.2)	54±2
4	10-10^2	hydroperoxides (multifunction.)	MALANHYOOH (, PINIC)	148±40	$k_{OH} = (0.05\text{-})1.5x10^{-10}$ J_{41} (MCMv3.2)	53±13
3	1-10	diols, multi-function. comp.	TLBIPER2OH	158±30	$k_{OH} = (1.2\pm0.8)x10^{-10}$ k_{NO3}: 10^{-11}-$2x10^{-10}$ k_{O3}: $(2\pm1.2)x10^{-18}$	72±20
2	0.1-1	dicarb. acids (dca)	CP02 (IOA)	150-200	$k_{OH} = (0.4\text{-}2.3)x10^{-11}$	120±30
1	0.01-0.1	multifunct. dca.	-"-	200-250	$k_{OH} = (0.4\text{-}2.3)x10^{-11}$	150±30

Table 4.

Atmospheric observations in Berlin used in this study linked to the responsible scientists. Most measurements were conducted in context of BAERLIN2014 campaign (Bonn et al., 2016; von Schneidemesser et al., 2017).

Parameter	*Resp. scientist*	*Location, site*
T, rH, NO, NO2, CO, benzene, toluene, PM_{10}, selected VOCs	A. von Stülpnagel, R. Nothardt (Senate Berlin, D)	MC042, Berlin-Neukoelln
global radiation	K. Müller (Free University, Berlin, D)	Botanical Garden, Berlin-Steglitz
selected VOCs (canister)	C. Kofahl, 2012 (RC Juelich, D)	MC042, Berlin-Neukoelln
selected VOCs (PTR-MS)	B. Bonn (IASS Potsdam, D)	MC042, Berlin-Neukoelln
mixing layer height	K. Schäfer (KIT, Garmisch-Partenkirchen, D)	MC042, Berlin-Neukoelln
T, wind	German Weather Service, Offenbach, D	00433, Airfield, Berlin-Tempelhof

Figure 1.

Effect of biogenic VOCs released by urban vegetation on ozone production.

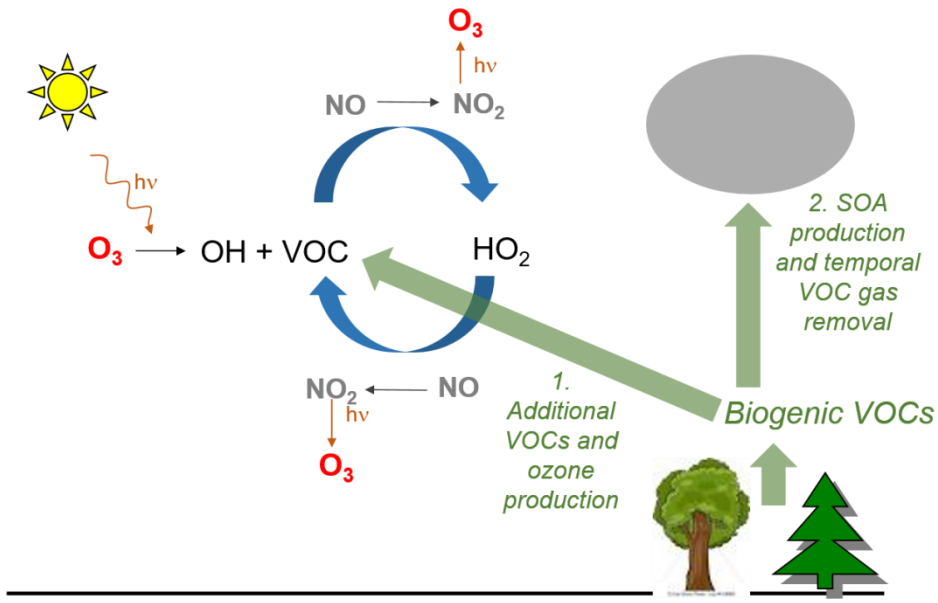


Figure 2.

Ozone comparison of reference simulation with observations on July 20th 2014 in Berlin, Germany. Observations are marked by dots and simulation results by a line.

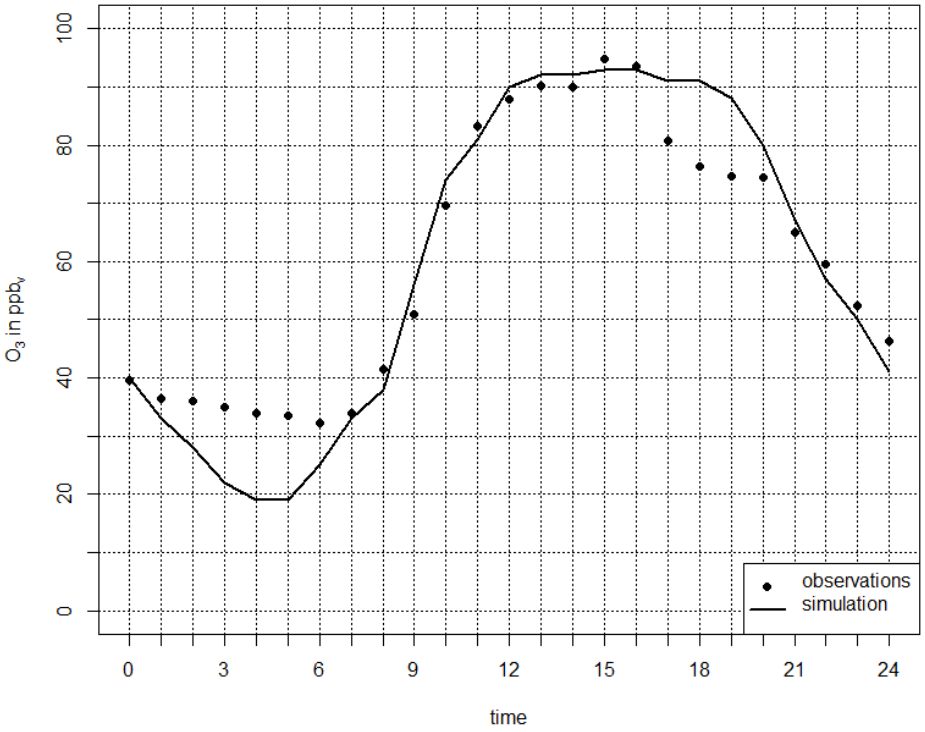


Figure 3.

Influence of isoprene (top) and monoterpenes (bottom) on ambient ozone mixing ratios. Note that the maximum daily isoprene and monoterpene mixing ratios of the single runs were plotted on the vertical axis. The colour scale refers to the ozone mixing ratio. It is different for both plots.

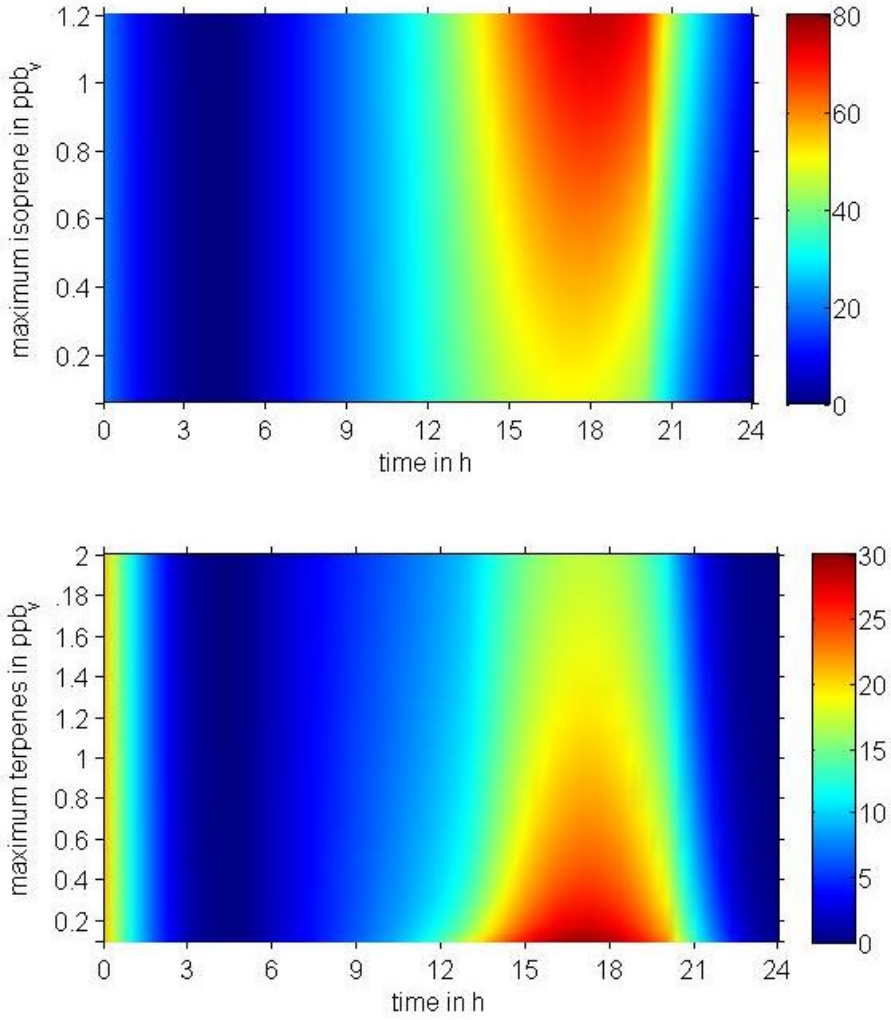


Figure 4.

Displayed is the simulated ozone mixing ratio vs. time with and without assuming different organic aerosol approaches using the idealized situation during CARES in Los Angeles. Major contribution at maximum was found for the SOA fraction with 70%.

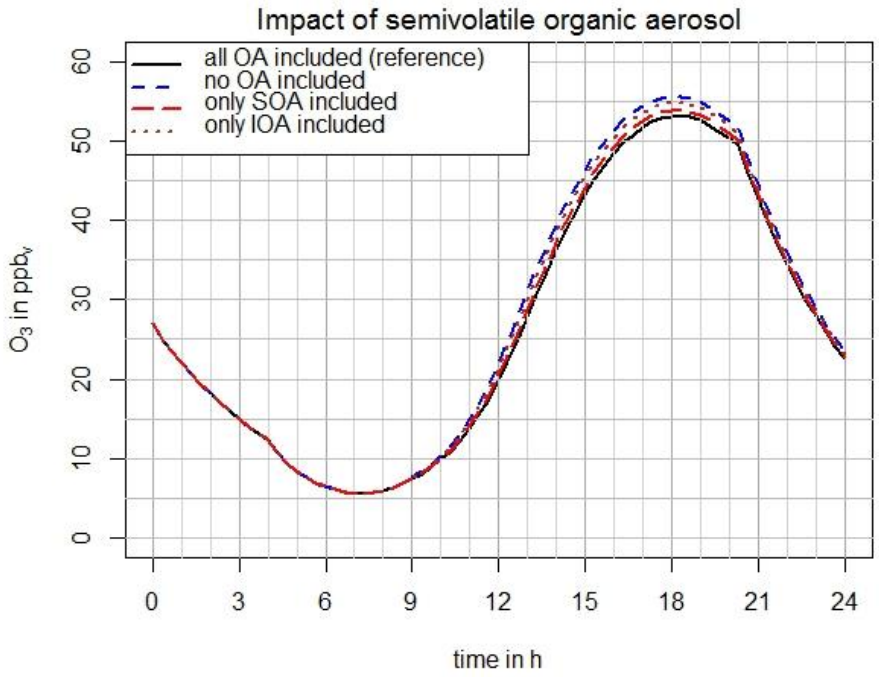


Figure 5.

Stacked contribution of volatility bin species to the ozone budget (mixing ratio) are plotted: As daily profile (left) and as relative contribution to the total effect of IOA at ozone maximum conditions (right). The species of the three most volatile bins 7, 8 and 9 represent more than 75% of the effect.

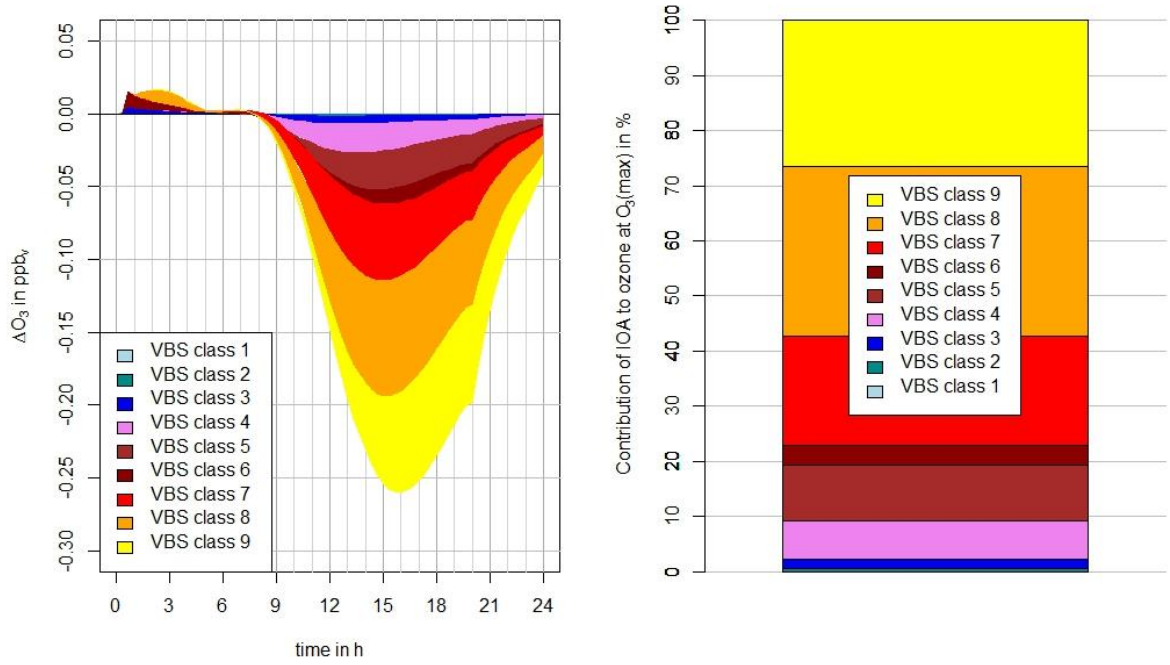
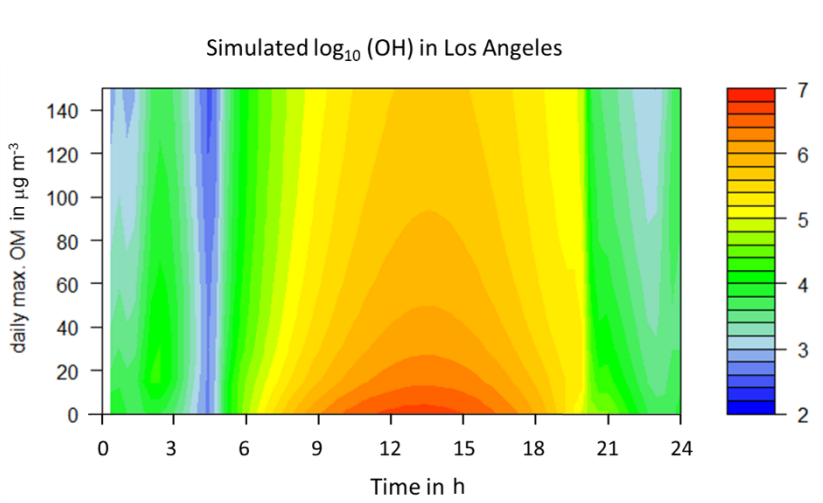
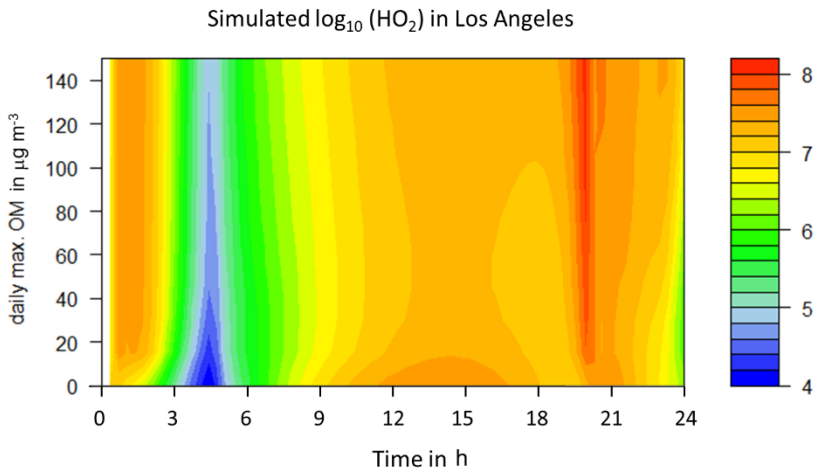


Figure 6.

Change of OH, HO_2 and ozone due to the presence of different initial amounts of IOA ($0.5*PM_{10}$) between 0 and 150 µg/m³. The ozone effect is related to the effects on HO_2.





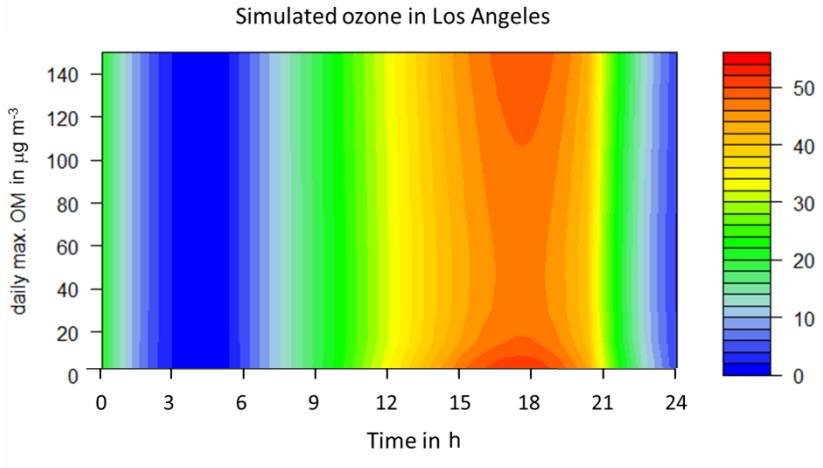


Figure 7.

Presented are contribution of different organic trace gases or groups to daily maximum ozone mixing ratio during June, July and August in Berlin (Germany). Different overall groups are displayed with different colours for easier identification.

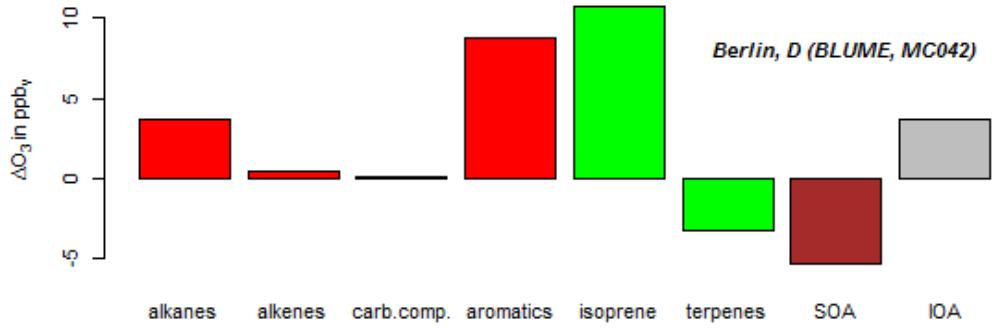


Figure 8.

Exemplary influence of changing tree species and their corresponding emissions on ambient ozone levels in Berlin. Upper: primary isoprene emitter (plane), centre: isoprene and monoterpene emitter (American sweetgum), and lower: primary monoterpene emitter (magnolia). The plots display the daily pattern vs. the contribution of a certain tree species to the current mixture. The simulated ozone levels are marked by colour.

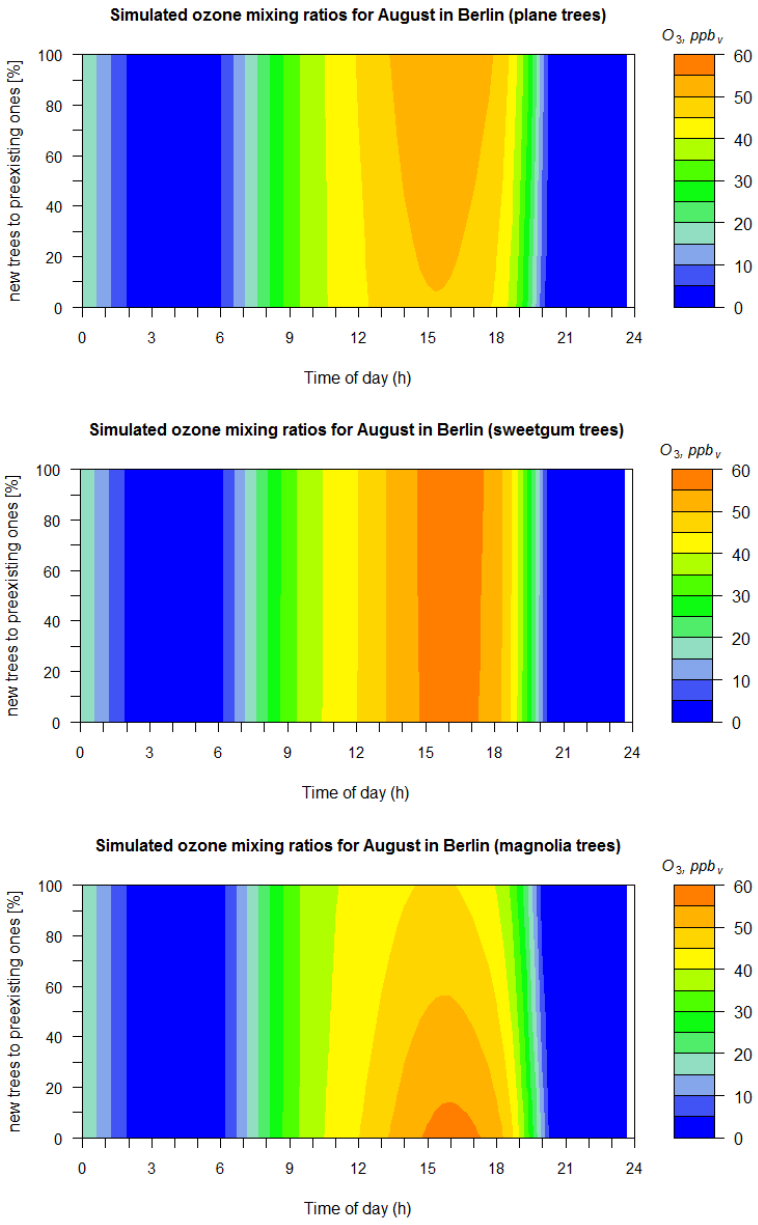


Figure 9.

Calculated ozone production rates $P(O_3)$ for different vegetation emissions of isoprene (E_{isop}, upper graph) and monoterpenes (E_{MT}, centre graph) at 35°C on July 20th in 2014. Individual data points reflect single tree species based emissions and resulting $P(O_3)$. The lowermost graph displays the comparison between fitted $P(O_3)$ and calculated $P(O_3)$.

